Electronic Supplementary Material (ESI) for ChemComm.

Electronic Supporting Information (ESI)

Site selectivity in the halogenation of titanium-functionalized polyoxovanadate-alkoxide clusters

Lauren E. VanGelder, Patrick L. Forrestel, William W. Brenessel, and Ellen M. Matson*

Department of Chemistry, University of Rochester, Rochester, New York 14627
Corresponding author email: matson@chem.rochester.edu

Supporting Information Table of Contents:

Experimental Details

General Considerations.

All manipulations were carried out in the absence of water and oxygen in a UniLab MBraun inert atmosphere glovebox under a dinitrogen atmosphere. Glassware was oven dried for a minimum of 4 hours and cooled in an evacuated antechamber prior to use in the drybox. Anhydrous methanol was purchased from Sigma-Aldrich and stored over activated 4 Å molecular sieves purchased from Fisher Scientific. All other solvents were dried and deoxygenated on a Glass Contour System (Pure Process Technology, LLC) and stored over activated 3 Å molecular sieves purchased from Fisher Scientific. $Ti(OCH_3)_4$, $AlCl_3$, and $AgSO_3CF_3$ were purchased from Sigma-Aldrich and used as received. $VO(OCH_3)_3$ was synthesized according to literature precedent.[1] Complex $[NBu_4][V_5O_6(OCH_3)_{12}(TiOCH_3)]$ (**1-V$_5$Ti**) was prepared according to literature procedures.[2, 3]

^{1}H NMR spectra were recorded at 500 on Bruker DPX-500 spectrometer locked on the signal of deuterated solvents. All chemical shifts were reported relative to the peak of residual ^{1}H signal in deuterated solvents. $CDCl_3$ was purchased from Cambridge Isotope Laboratories, degassed by three freeze−pump−thaw cycles, and stored over activated 4 Å molecular sieves. Infrared (FT-IR, ATR) spectra of complexes were recorded on a Shimadzu IRAffinity-1 Fourier Transform Infrared Spectrophotometer and are reported in wavenumbers (cm^{-1}). Electronic absorption measurements were recorded at room temperature in anhydrous acetonitrile in a sealed 1 cm quartz cuvette with an Agilent Cary 60 UV-Vis spectrophotometer. Mass spectrometry analyses were performed on an Advion expression^L Compact Mass Spectrometer equipped with an electrospray probe and an ion-trap mass analyzer. Direct injection analysis was employed in all cases with a sample solution in acetonitrile. Single crystals were mounted on the tip of a thin glass optical fiber (goniometer head) and mounted on a Bruker SMART APEX II CCD platform diffractometer for a data collection at 100.0(5) K. The structures were solved using SHELXT-2014/5[4] and refined using SHELXL-2014/7.[5] Elemental analyses were performed on a PerkinElmer 2400 Series II Analyzer, at the CENTC Elemental Analysis Facility, University of Rochester.

Synthesis of [$V_4O_5(OCH_3)_{12}(TiOCH_3)_2$] (2-$V_4Ti_2$)

In the glovebox, $VO(OCH_3)_3$ (0.900 g, 5.624 mmol) and 28 mL MeOH were charged in a 50 mL Teflon-lined Parr reactor. $Ti(OCH_3)_4$ (0.484 g, 2.814 mmol) was added as a solid to the reaction mixture. The Parr reactor was sealed, and the mixture heated in an oven at 125 ^oC for 72 hours. The Parr reactor was allowed to cool to room temperature, then returned to the glove box. The reaction yielded a red brown solution with a dark red crystalline precipitate. The mother liquor was decanted, after which the crystals were washed with Et_2O (10 mL, 3x). Solvent was removed under vacuum and these crystals were used for X-ray analysis. The mother liquor was dried under vacuum, dissolved in a minimal amount of hot MeOH (2 mL), filtered, and cooled to −30 ^oC for 24 hours. Additional red crystals precipitate from this solution. The mother liquor was decanted, the crystals washed with Et_2O (10 mL, 3x), and these crystals were added to those which formed directly from the reaction mixture to yield pure **2-V_4Ti_2** (1.048 g, 1.294 mmol, 92%). ^1H NMR (500 MHz, $CDCl_3$) δ = 0.94, 2.83, 3.89, 6.51, 11.56, 13.04, 27.58 ppm. FT-IR (ATR, cm^{-1}): 978.9, 1031.9, 1130.3, 1444.7. UV−Vis (CH_3CN) [ε (M^{-1} cm^{-1})]: 428 nm (745), 684 nm (117). Elemental analysis: Calculated (%) for (MW = 813.97 g/mol): C, 20.66; H, 5.20 %. Found: C, 20.798; H, 5.087 %.

Synthesis of [NBu_4][$V_5O_6(OCH_3)_{12}TiCl$] (3-V_5TiCl)

In the glovebox, **1-V_5Ti** (0.200 g, 0.192 mmol) was dissolved in DCM (7 mL). To this was added a solution of $AlCl_3$ (0.025 g, 0.192 mmol) in DCM (5 mL). The resulting solution was allowed to stir at room temperature for 24 hours, after which any residual solid was filtered out and the solution evaporated to dryness. This resulting solid was washed with pentane (3x, 10 mL) and ether (3x, 10 mL), giving the desired compound **3-V_5TiCl** as a brown-yellow oily solid (0.122 g, 0.130 mmol, 67.7%). ^1H NMR (500 MHz, $CDCl_3$) δ = 1.00, 1.42, 3.18, 5.29, 13.86, 15.97, 20.80, 30.54 ppm. FT-IR (ATR, cm^{-1}): 968.2, 1006.8, 1141.8, 1168.9, 1425.4, 1440.8. UV−Vis (CH_3CN) [ε (M^{-1} cm^{-1})]: 383 nm (2,471), 648 nm (191). Elemental analysis: Calculated (%) for (MW = 1048.89 g/mol): C, 32.06; H, 6.92; N, 1.34 %. Found: C, 32.567; H, 6.567; N, 0.959 %.

Synthesis of [$V_3O_4(VCl)(OCH_3)_{12}(TiOCH_3)_2$][$AlCl_4$] (4-$V_3Ti_2VCl$)

In the glovebox, **2-V_4Ti_2** (0.200 g, 0.246 mmol) was dissolved in DCM (7 mL). To this was added a solution of $AlCl_3$ (0.098 g, 0.737 mmol) in DCM (5 mL). The resulting mixture was allowed to stir for 48 hours, after which any residual solid was filtered out, and the solution evaporated to dryness. The resulting solid was washed with ether (3x, 10 mL), giving the desired product **4-V_3Ti_2VCl** (0.151 g, 0.182 mmol, 74.0%)**.** X-ray quality crystals were grown from a saturated solution of **4-V_3Ti_2VCl** in THF, cooled to -35 ^oC overnight. ^1H NMR (500 MHz, $CDCl_3$) δ = -24.28, -15.25, 5.35, 5.87, 12.47, 16.13, 20.59 ppm. FT-IR (ATR, cm^{-1}): 682.8, 844.8, 852.5, 1003.0, 1103.3, 1172.7, 1242.2, 1342.5, 1440.8. Elemental analysis: Calculated (%) for (MW = 1110.38 g/mol): C, 21.63; H, 4.9 %. Found: C, 21.750; H, 4.866 %.

Table S1. Crystallographic parameters for molecular structure of **1-V$_5$Ti, 2-V$_4$Ti$_2$,** and **4-Ti$_2$V$_4$Cl**

Compound	**1-V$_5$Ti** **CCDC 1587541**	**2-V$_4$Ti$_2$** **CCDC 1820423**	**4-Ti$_2$V$_4$-Cl** **CCDC 1825306**
Empirical formula	$C_{29}H_{75}O_{19}V_5Ti$	$C_{14}H_{42}O_{19}Ti_2V_4$	$C_{20}H_{54}AlCl_5O_{19.5}Ti_2V_4$
Formula weight	1044.50	814.03	1110.42
Temperature / K	100.0(5)	100.0(5) K	100.0(5) K
Wavelength / Å	0.71073	0.71073	0.71073
Crystal system	Monoclinic	Monoclinic	Monoclinic
Space group	$P2_{1/c}$	$P2_{1/n}$	$P2_{1/m}$
Unit cell dimensions	a = 11.5947(17) Å b = 18.157(3) Å c = 23.178(3) Å α = 90° β = 103.2149(18)° γ = 90°	a = 10.2851(10) Å b = 24.103(2) Å c = 12.0280(12) Å α = 90° β = 92.176(2)° γ = 90°	a = 19.3992(19) Å b = 11.6179(11) Å c = 19.5185(19) Å α = 90° β = 96.728(2)° γ = 90°
Volume / Å^3	4750.3(12) Å^3	2979.6(5) Å^3	4368.7(7) Å^3
Z	4	4	4
Reflections collected	51687	73818	110728
Independent reflections	8626	16343	13948
Completeness (theta)	100.0% (25.242°)	99.8% (37.785°)	99.9% (30.508°)
Goodness-of-fit on F^2	1.009	1.036	1.037
Final R indices [I>2sigma(I)]	R1 = 0.0692	R1 = 0.0503	R1 = 0.0582
Largest diff. peak and hole	0.526 & -0.693 Å^{-3}	1.488 & -1.014 Å^{-3}	1.971 & -1.239 Å^{-3}

Figure S1. Electrospray-ionization mass spectrum of **2-V$_4$Ti$_2$** (+*ve*). Predicted spectrum (top) and raw data (bottom). Experimental isotope distribution matches that expected for a di-titanium POV-alkoxide.

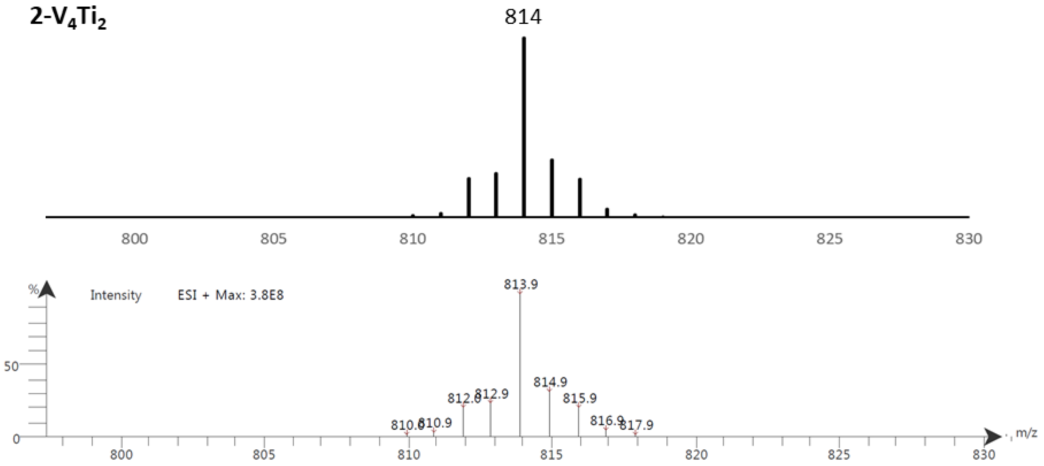

Figure S2. ^{1}H NMR of **1-V$_5$Ti**, **2-V$_4$Ti$_2$** and V$_6$O$_7$(OCH$_3$)$_{12}$ in CDCl$_3$. The ^{1}H NMR spectrum of **1-V$_5$Ti** shows three prominent resonances in the paramagnetic region (11.56, 13.04, and 27.58 ppm), indicative of a loss in symmetry as compared to the previously reported clusters, [V$_6$O$_7$(OCH$_3$)$_{12}$] and **1-V$_5$Ti**.[3, 6]

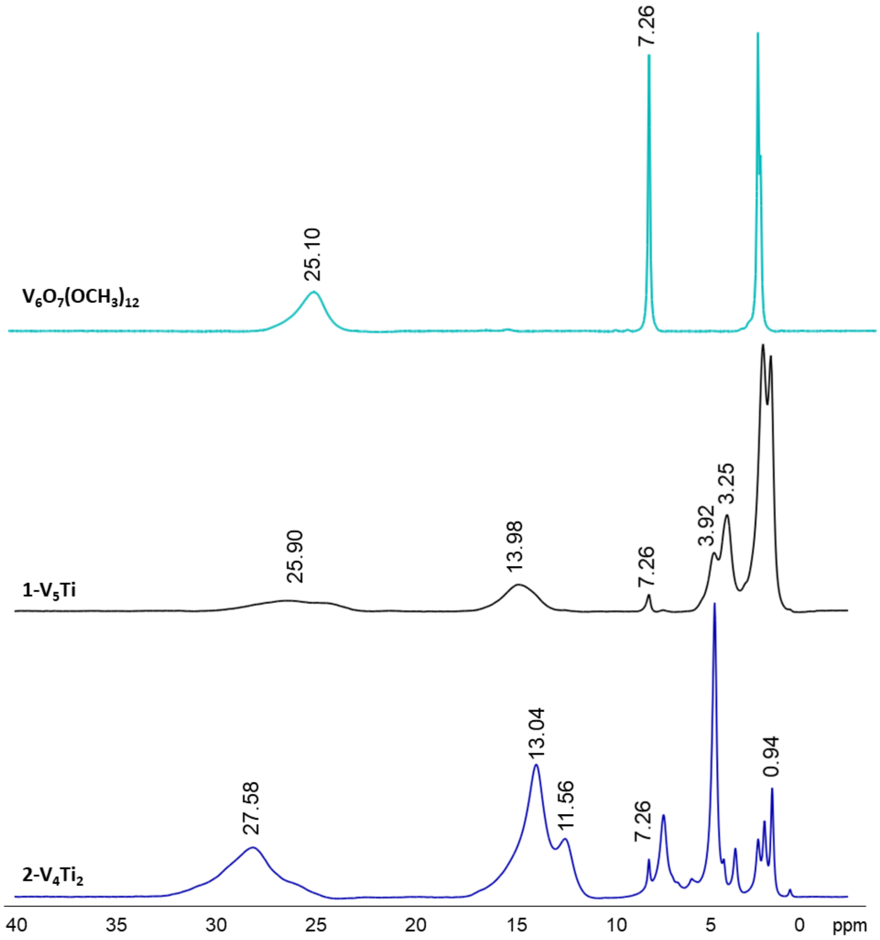

Figure S3. Infrared absorption spectra of **1-V$_5$Ti** and **2-V$_4$Ti$_2$**. The two strong absorbance bands in the spectrum of **2-V$_4$Ti$_2$** correspond to ν(V=O$_t$) (O$_t$ = terminal oxo; 979 cm^{-1}) and ν(O$_b$-CH$_3$) (O$_b$ = bridging oxo; 1032 cm^{-1}) stretching frequencies, confirming the formation of the desired Lindqvist core.[7] A third feature is observed at 1130 cm^{-1}, assigned to ν(TiO-CH$_3$), consistent with that reported for the terminal titanium methoxide moiety in complex **1-V$_5$Ti** (ν(TiO-CH$_3$): 1152 cm^{-1}).

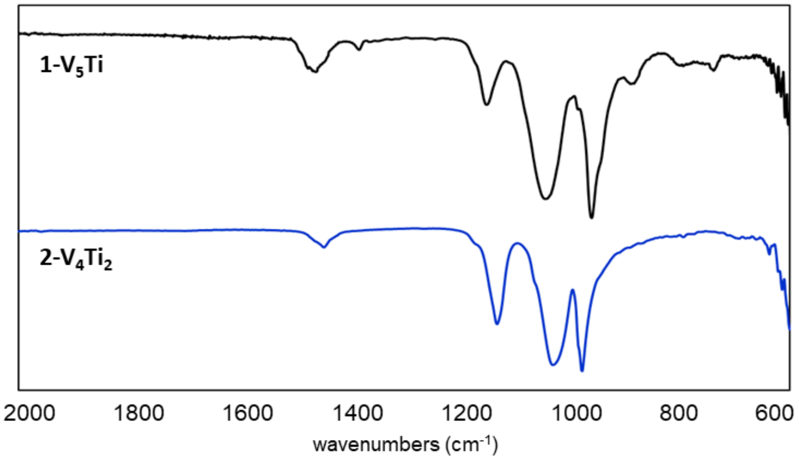

Figure S4. UV-vis absorption spectra of **1-V$_5$Ti**, **2-V$_4$Ti$_2$**, and V$^{IV}_6$O$_7$(OCH$_3$)$_{12}$ in acetonitrile. The absence of IVCT absorbance features in the spectrum of **2-V$_4$Ti$_2$**, combined with the presence of a weak absorption at 684 nm (ε = 117 M^{-1}cm^{-1}), suggests an isovalent, V^{IV} electron configuration for the four vanadium ions.[6, 8, 9] In the absorption spectrum of **2-V$_4$Ti$_2$**, the broad feature located at 428 nm (ε = 745 M^{-1}cm^{-1}), attributed to the intervalence electron transfer from a d^1, V^{IV} ion to a d^0 Ti^{IV} centre,[15] is substantially more intense relative to **1-V$_5$Ti** (ε = 745 vs. 579 M^{-1}cm^{-1}, respectively).[6] This is consistent with the greater number of titanium centres in complex **2-V$_4$Ti$_2$**, which increases the probability of occurrence of a charge transfer event between the vanadium and titanium centres.

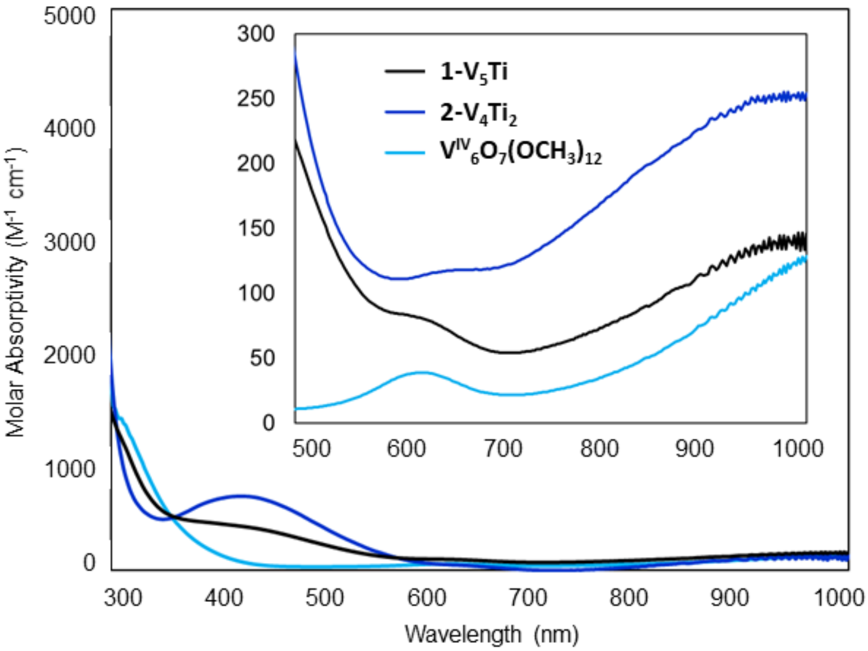

Figure S5. Electrospray-ionization mass spectrum of **3-V$_5$TiCl** (−*ve*). Peak at *m/z* = 806/808 is consistent with formation of [NBu$_4$][V$_5$O$_6$(OCH$_3$)$_{12}$TiCl] (**3-V$_5$TiCl**) Peak at *m/z* = 939 is consistent with the capping of **3-V$_5$TiCl** with excess AlCl$_3$.

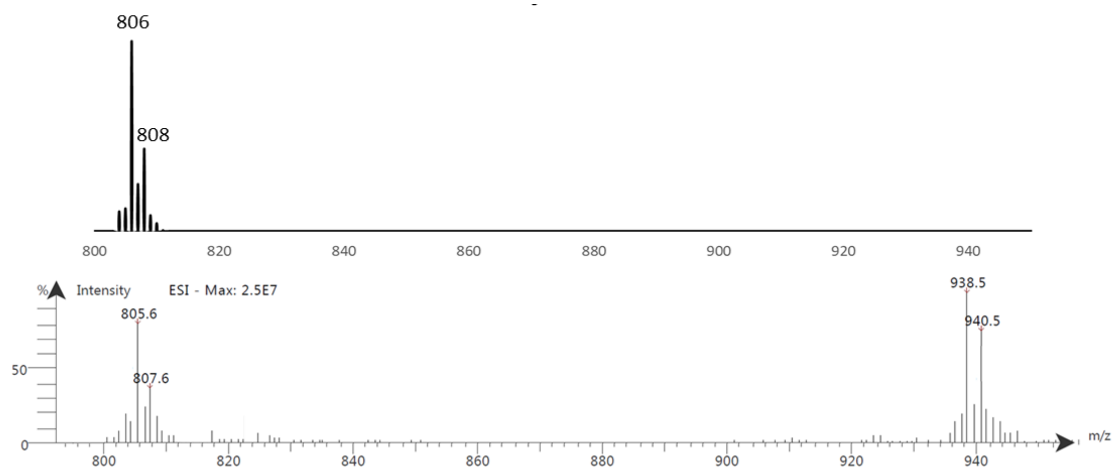

Figure S6. ^{1}H NMR of **1-V$_5$Ti** and **3-V$_5$TiCl** in CDCl$_3$.

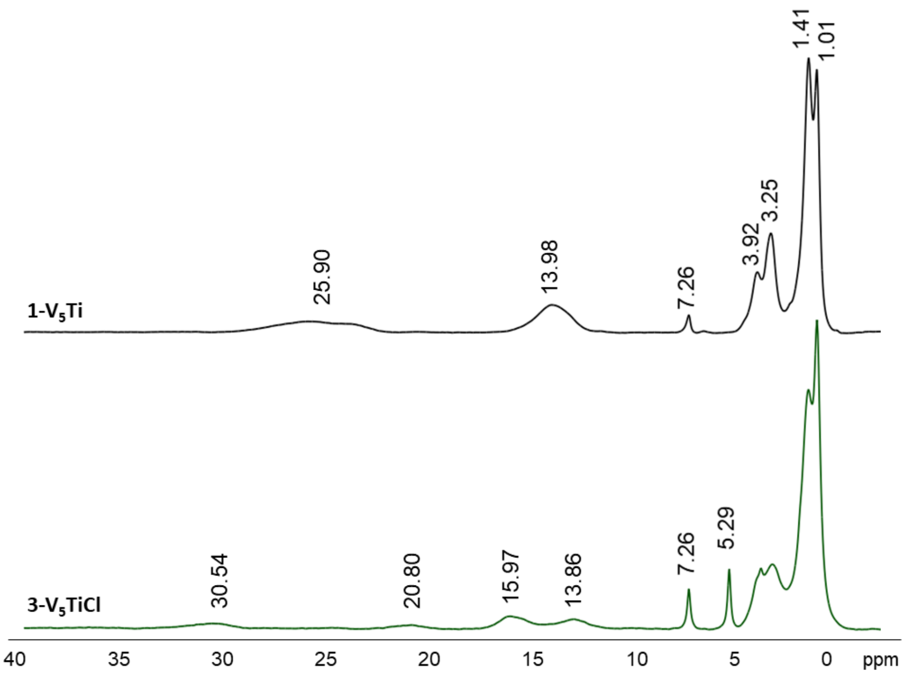

Figure S7. Infrared absorption spectroscopy of **1-V_5Ti** and **3-V_5TiCl**. The loss of the strong feature assigned to *v*(TiO-CH_3) (1152 cm^{-1}) corresponds to the substitution of the terminal methoxide ligand with a chloride ion, resulting in the generation of a Ti-Cl bond.

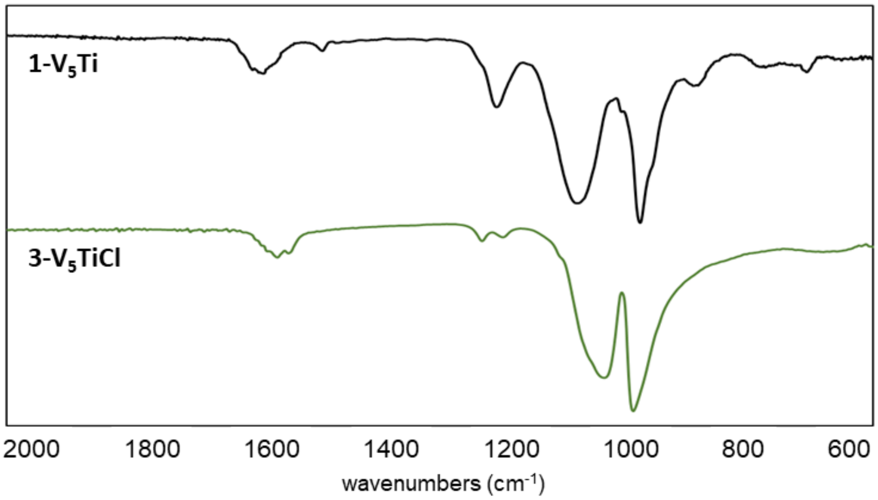

Figure S8. UV-vis absorption spectra of **1-V_5Ti**, **3-V_5TiCl**, and $V^{IV}{}_5V^{V}{}_1O_7(OCH_3)_{12}$ in acetonitrile.

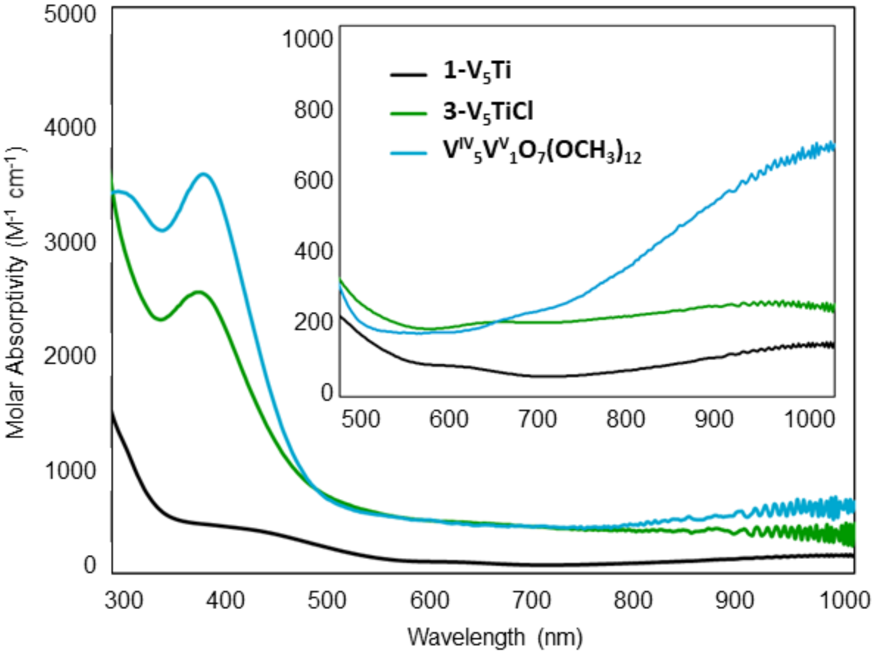

Figure S9. Electrospray-ionization mass spectrum of **4-V_3Ti_2VCl** (+ *ve*)

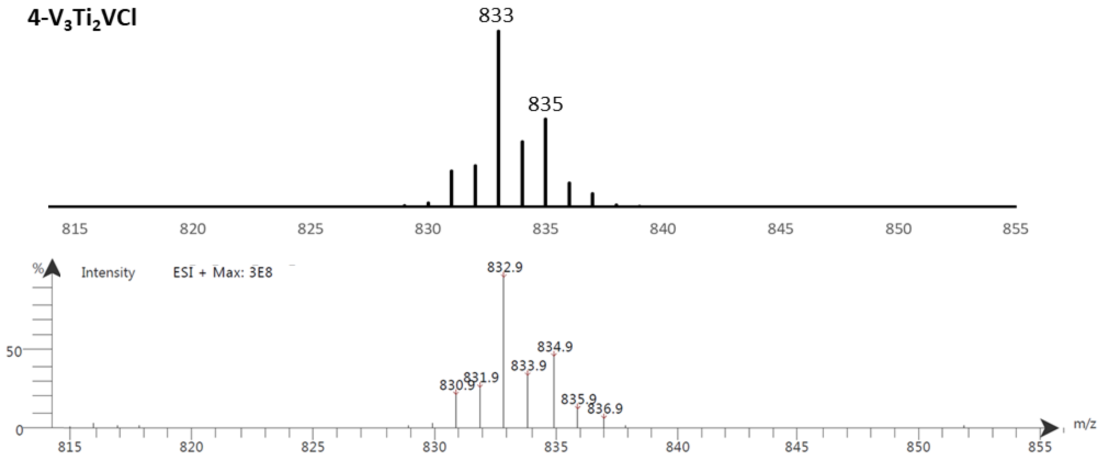

Figure S10. ^1H NMR of **2-V_4Ti_2** and **4-V_3Ti_2VCl** in $CDCl_3$.

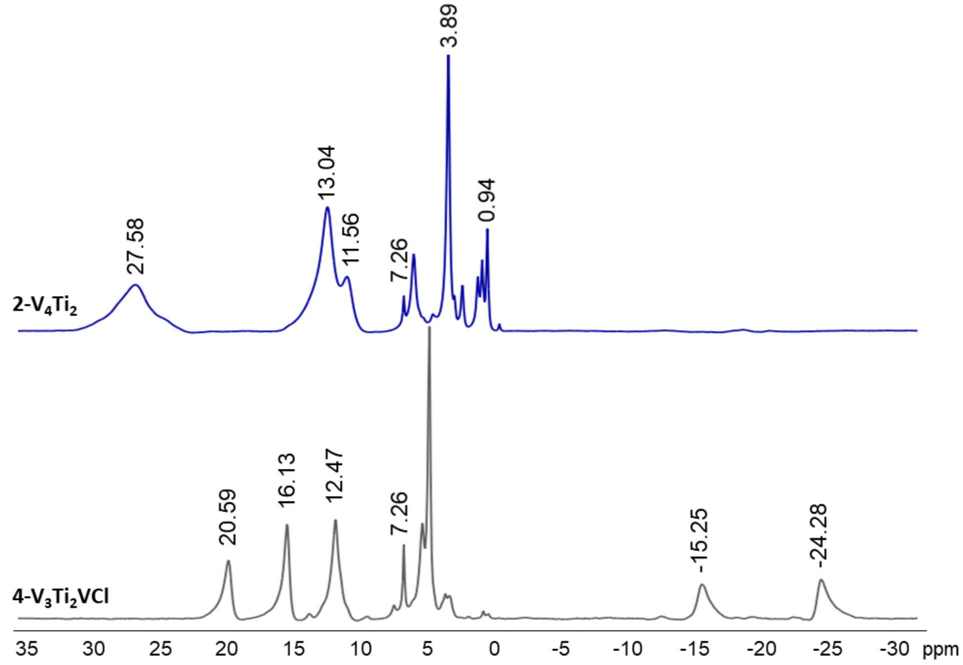

Figure S11. Infrared absorption spectra of **$2\text{-}V_4Ti_2$** and **$4\text{-}V_3Ti_2VCl$**. In the spectrum of **$4\text{-}V_3Ti_2V\text{-}Cl$**, we observe retention of the *v*(Ti-OCH_3) stretching frequency (1173 cm^{-1}), supportive of the resistance of the Ti-O_m linkages to chlorination. The lack of *v*(V=O_t) and *v*(O_b-OCH_3) stretching frequencies (which are characteristic of delocalized POV-alkoxides) suggests a disruption in the delocalization of the cluster core.

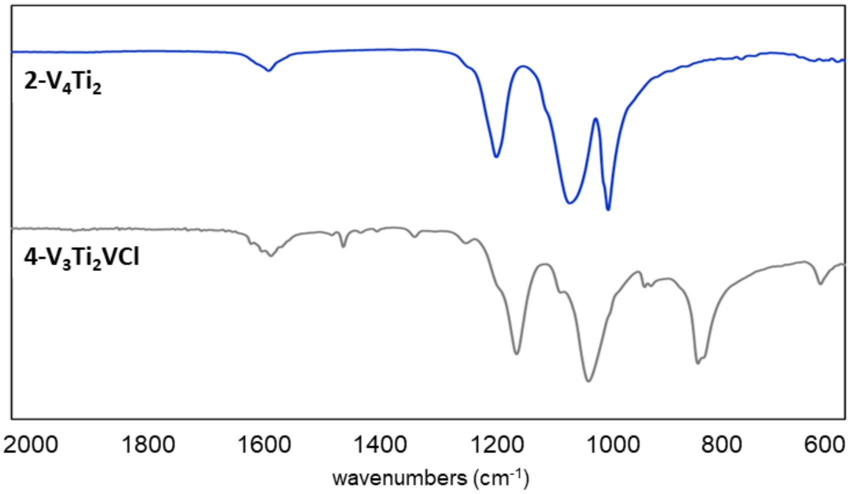

Figure S12. UV-vis absorption spectra of **$2\text{-}V_4Ti_2$**, **$4\text{-}V_3Ti_2VCl$**, and $V^{IV}_6O_7(OCH_3)_{12}$ in acetonitrile. The spectrum of **$4\text{-}V_3Ti_2VCl$** shows none of the features observed in the spectrum of **$2\text{-}V_4Ti_2$**, supporting the disruption in the electronic delocalization suggested by the ^1H NMR and IR spectra.

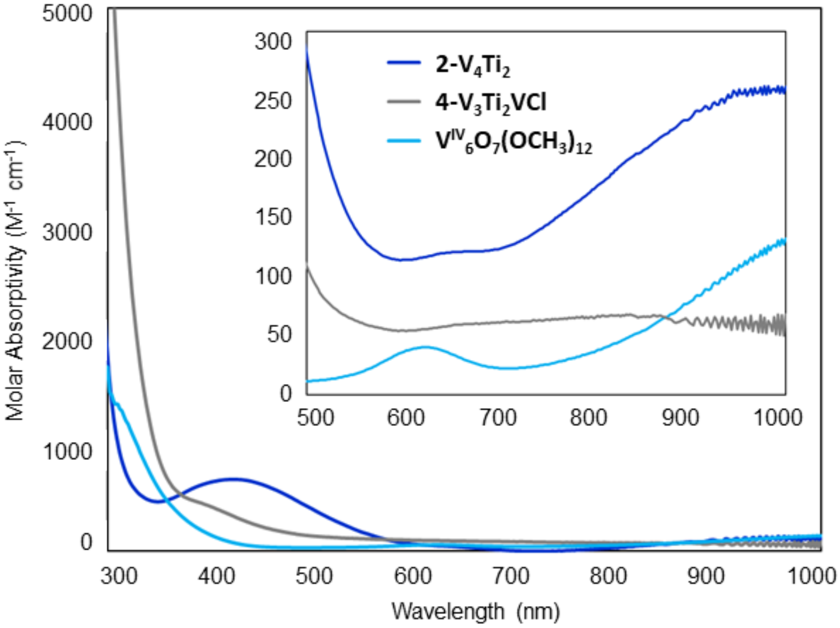

Figure S12. Chlorination of **1-V$_5$Ti** and **2-V$_4$Ti$_2$** using TiCl$_4$ as the halogen source. Analogous procedures were used to those with AlCl$_3$ as the chloride source. (a) Electrospray-ionization mass spectrum of **3-V$_5$TiCl** resulting from this reaction (−*ve*). ESI-MS shows the expected peak (*m/z* = 806/808) (b) Electrospray-ionization mass spectrum of **4-V$_3$Ti$_2$VCl** resulting from this reaction (+*ve*). ESI-MS shows the expected peak (*m/z* = 833).

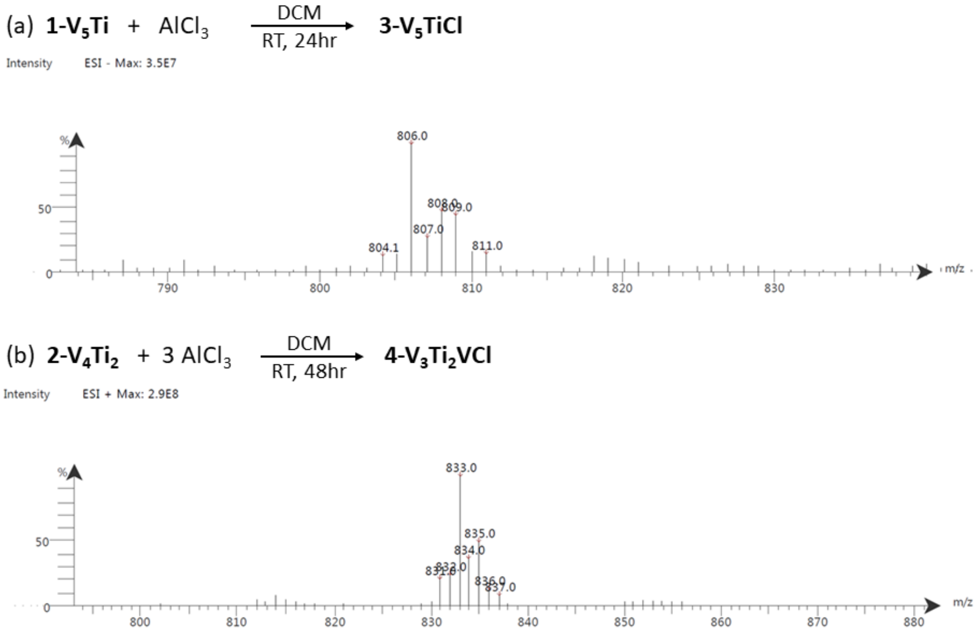

Figure S13. Probing the reversibility of the chlorination of **1-V$_5$Ti**. Electrospray-ionization mass spectrum resulting from this reaction (−*ve*) shows a peak only at (*m/z* = 802), indicating reversible formation of **1-V$_5$Ti** from **3-V$_5$TiCl**.

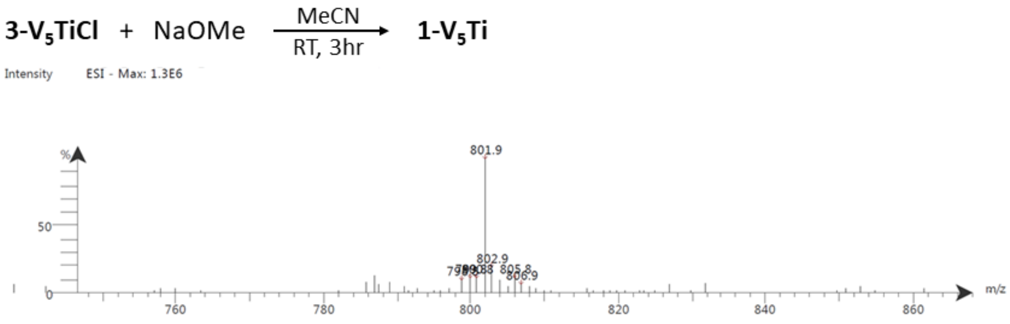

Figure S14. Probing the reversibility of the chlorination of **2-V$_4$Ti$_2$**. Electrospray-ionization mass spectrum resulting from these reactions (+*ve*) show a peak only at (*m/z* = 833), indicating that the V-Cl chloride is not substituted for an oxygen moeity under these reaction conditions.

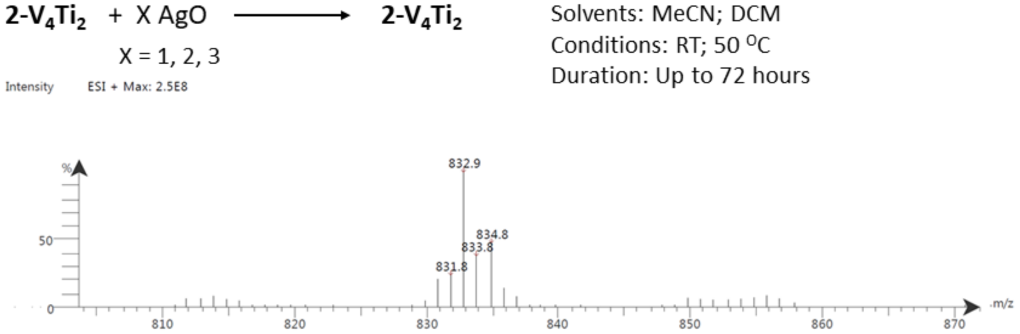

References:

1. C. Daniel and H. Hartl, *Journal of the American Chemical Society*, 2009, **131**, 5101-5114.
2. L. E. VanGelder, W. W. Brennessel and E. M. Matson, *Dalton Transactions*, 2018, **47**, 3698-3704.
3. J. Spandl, C. Daniel, I. Brüdgam and H. Hartl, *Angewandte Chemie International Edition*, 2003, **42**, 1163-1166.
4. G. M. Sheldrick, *SHELXT-2014/5*.
5. G. M. Sheldrick, *Acta Crystallographica Section C*, **71**, 3-8.
6. L. E. VanGelder, W. W. Brennessel and E. M. Matson, *Dalton Transactions*, 2018, DOI: 10.1039/C7DT04455K.
7. L. E. VanGelder, A. M. Kosswattaarachchi, P. L. Forrestel, T. R. Cook and E. M. Matson, *Chemical Science*, 2018, **9**, 1692-1699.
8. F. Li, S. H. Carpenter, R. F. Higgins, M. G. Hitt, W. W. Brennessel, M. G. Ferrier, S. K. Cary, J. S. Lezama-Pacheco, J. T. Wright, B. W. Stein, M. P. Shores, M. L. Neidig, S. A. Kozimor and E. M. Matson, *Inorganic Chemistry*, 2017, **56**, 7065-7080.
9. A. Müller, J. Meyer, H. Bögge, A. Stammler and A. Botar, *Zeitschrift für anorganische und allgemeine Chemie*, 1995, **621**, 1818-1831.